Mem. S.A.It. Suppl. Vol. 18, 109

Memorie della
Supplementi

Pattern speeds in interacting galaxies

C. L. Dobbs

Department of Physics, University of Exeter, Exeter, UK
e-mail: dobbs@astro.ex.ac.uk

Abstract. We investigate pattern speeds in spiral galaxies where the structure is induced by an interaction with a companion galaxy. We perform calculations modeling the response of the stellar and/or gaseous components of a disc. Generally we do not find a unique pattern speed in these simulations, rather the pattern speed decreases with radius, and the pattern speed for individual spiral arms differ. The maximum pattern speed is ~20 km s^{-1} kpc^{-1} for the discs with a live stellar component, decreasing to 5 km s^{-1} kpc^{-1} at the edge of the spiral perturbation. When only the gas is modeled, $\Omega_{\rm p}$ is typically very low (5 km s^{-1} kpc^{-1}) at all radii.

Key words. galaxies: kinematics and dynamics – galaxies: interactions – galaxies: spiral – galaxies: structure – hydrodynamics – stellar dynamics

1. Introduction

Most grand design spiral patterns are believed to be due to interactions with other galaxies (Toomre & Toomre 1972), or are driven by bars (Kormendy & Norman 1979; Bottema 2003, Athanassoula et al., this volume). Here we investigate the first of these scenarios, by performing numerical simulations of interacting galaxies. In this instance, there is not necessarily a singular pattern speed for the spiral arms, as indicated by recent observations of M51 (Meidt et al. 2008a).

2. Method

We use the Smoothed Particle Hydrodynamics Code (SPH) to model a galaxy subject to an interaction. The first galaxy is modeled by assuming a spherical potential for the halo, with 3 different scenarios for the galactic disc: a) a live stellar disc, no gas; b) a logarithmic stellar potential and a live gaseous disc and c) a disc containing live gaseous and stellar components. The stars and/or gas are allocated velocities such that the Toomre instability parameter, Q, is globally 2, but in addition, the galaxy was allowed to evolve in isolation until any flocculent structure disappears. In all simulations 1 million particles are used. For the case of stars and gas there are 500,000 gas particles and 500,000 stellar particles, and in all cases the total mass of the disc is 5×10^9 M$_\odot$.

We adopt a similar approach to Oh et al. (2008) to model the interaction. The interacting galaxy is represented by a sink particle (Bate et. al. 1995) and is of relatively low mass, equal to the mass of the disc or 2.5% of the total mass of the first galaxy. The interacting galaxy takes a parabolic orbit, reaching a closest approach of 25 kpc after a time of 370 Myr. Initially this galaxy is at a distance of 50 kpc.

Send offprint requests to: Clare L. Dobbs

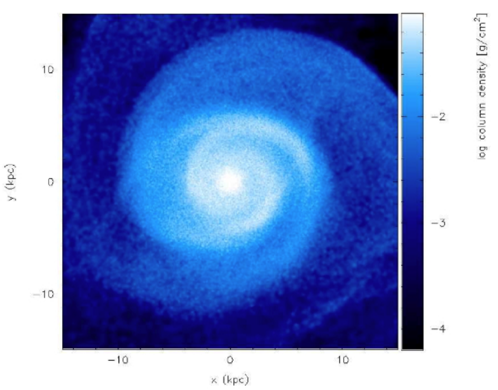

Fig. 1. The column density is shown for a stellar disc of a galaxy perturbed by a (point mass) galaxy on a parabolic orbit. The second galaxy is located 70 kpc away, at the coordinates $(-20, 68)$ kpc. The stellar disc contains broad and diffuse spiral arms.

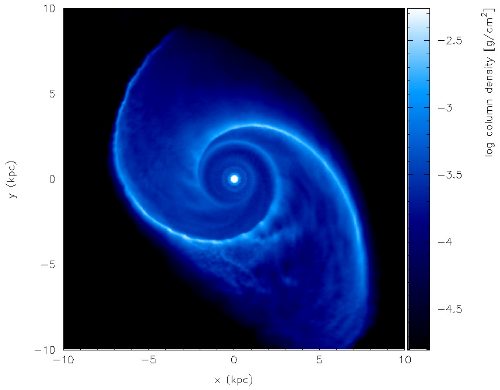

Fig. 3. The column density is shown for the gas disc perturbed by a galaxy, at the same time as Fig. 1. The gas shocks produce very narrow, dense spiral arms compared to Fig. 1.

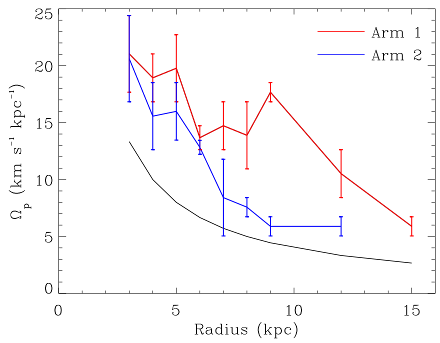

Fig. 2. The pattern speeds for each spiral arm are plotted versus radius for the stellar disc. Ω_p is different for each arm and decreases with radius. The lower line shows a $1/r$ dependence.

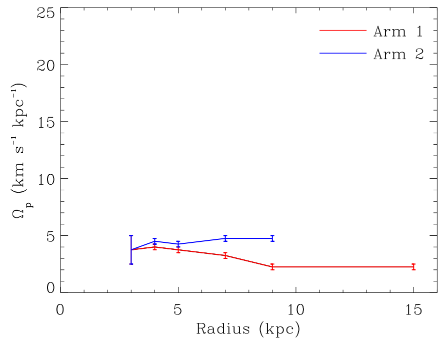

Fig. 4. The pattern speeds are plotted for the spiral arms of the gas disc. Ω_p is much lower than typical from observations.

3. Results

3.1. Stellar disc

Fig. 1 shows the column density of a stellar disc, at a time of 820 Myr. The interacting galaxy is 70 kpc from the centre of the plot. The spiral arms are relatively weak and broad.

We calculate the pattern speed of the spiral arms according to

$$\Omega_p = \frac{\phi(\rho_{max})|_{t_2} - \phi(\rho_{max})|_{t_1}}{t_2 - t_1} \quad (1)$$

where ρ_{max} is the peak density of a particular spiral arm at a given radius, and t_1 and t_2 are times during the simulation. First we select points covering a particular spiral arm at time $t_1 = 800$ Myr, when a strong spiral pattern has emerged. Then the azimuthal angle of the spiral arm is located for different radii. This process is repeated at time $t_2 = 925$ Myr, to obtain the change in azimuthal angle of the spiral arm at each radius, and thus Ω_p. Given there are 2 spiral arms, this method leads to a pattern speed for each spiral arm. These pattern speeds are shown versus radius in Fig. 2, the errors reflecting the uncertainty in locating the peak density of the spiral arm.

The magnitude of the pattern speeds are not dissimilar from some of those measured for spirals (e.g., Clemens & Alexander 2001; Grosbøl et al. 2006), although the spiral arms clearly exhibit different pattern speeds. This difference is a consequence of the asymmetry of the system, i.e. that the interaction induces one arm on one side of the disc first. The pattern speeds for each arm also decrease with radius, roughly as expected for spiral patterns induced by interactions.

3.2. Gaseous disc

We also performed calculations with just gas. The gas constitutes 1% of the mass of the galactic disc. This value is unrealistically small, but the low gas mass is chosen to avoid gravitational instabilities, which would halt the calculation. Essentially, we are only investigating the reaction of the gas to the interaction, not the self gravity of the gas. These calculations are also not a particularly realistic case as they ignore the perturbation experienced by the stellar disc from the interaction (instead the stellar disc is represented by a symmetric potential). However the case with just gas is explored for completeness.

In Fig. 3, we show the disc when only the gas is included, at the same time (800 Myr) as Fig. 1. The spiral arms are clearly much narrower, more prominent, and more dense than for the stellar disc. The evolution of the gas and stellar discs is also different. The gaseous spiral arms rotate much slower than the stellar arms. Consequently the pattern speed is very low, ~4 km s^{-1} kpc^{-1} and does not show much variation with radius (Fig. 4). The difference compared to the stellar disc is that one spiral arm is still linked to, and rotates at the same angular velocity as, the orbiting galaxy.

3.3. Evolving both the stars and gas

Finally we show calculations with gas and stars, again where the gas represents 1% of the mass of the stellar disc. Thus the mass of

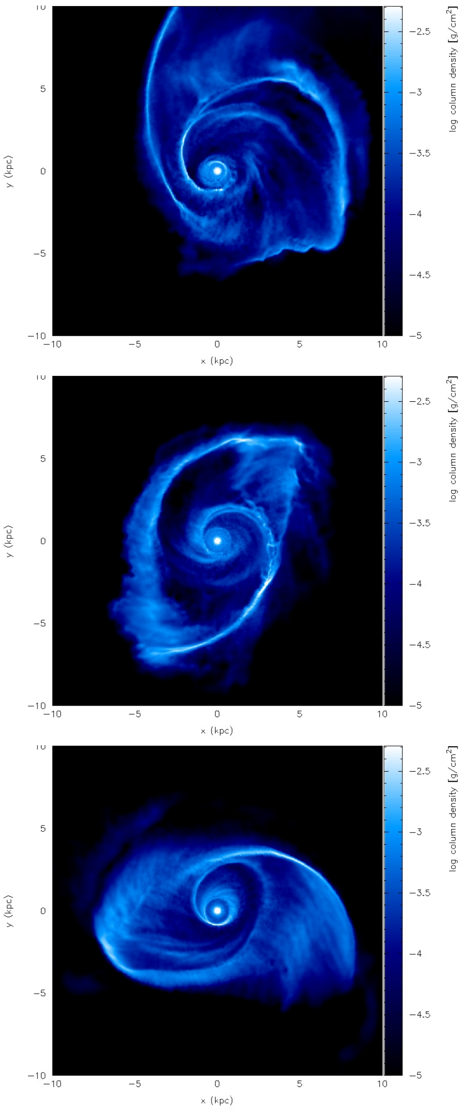

Fig. 5. The gas distribution is shown from a calculation with gas and stars at times of 500 (top), 740 (middle) and 1060 Myr (bottom). The spiral arms are very asymmetric at the earliest time (when the position of the interacting galaxy is located at (22.5, 15) kpc), but becomes more symmetric at later times, after the interaction.

the stellar disc is 5×10^9 $M_\odot$ and the gaseous disc 5×10^8 $M_\odot$, although the actual number of gas and stellar particles in the calculation are equal. Fig. 5 shows the column den-

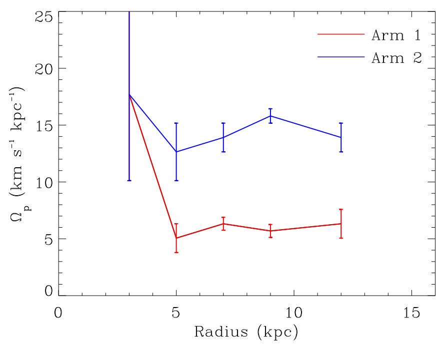

Fig. 6. The pattern speed is shown for the gaseous arms, from the simulation with stars and gas. The gas is largely coupled to the stars, hence Ω_p is higher than when only gas particles are present. Again there is a clear difference in the pattern speeds of each spiral arm.

sity of gas from the calculation with live stellar and gaseous components. The morphology evidently changes over time. At an earlier stage in the interaction, the spiral pattern is very asymmetric (unlike the calculations with gas alone, where the spiral pattern is symmetric throughout the simulation). The pattern becomes more symmetric at later times, tending towards the distribution without a live stellar disc (Fig. 3). Although not shown on Fig. 5, the stellar distribution reflects the gas distribution, but the spiral arms are much weaker and broader.

Finally in Fig. 6 we plot the pattern speed of the gas from the calculation with both live stellar and gaseous components. The times selected to calculate the pattern speed are 450 and 500 Myr. The spiral arms clearly have very different pattern speeds, which is not surprising given the asymmetry of the disc. The spiral arm with the lower pattern speed is still associated with the interacting galaxy. The pattern speeds are more similar in magnitude to the case when only stars are used (Fig. 2), since the gas is better coupled to the stars.

4. Conclusions

We have performed calculations with a stellar, gaseous and both stellar and gaseous disc subject to an interaction with an orbiting galaxy. The pattern speed across the disc is generally not constant, and pattern speeds in each arm differ. For a stellar disc, $\Omega_p = 5 - 20$ km s^{-1} kpc^{-1}, decreasing with radius approximately as $1/r$. With only gas, the pattern speeds are much lower ($3-6$ km s^{-1} kpc^{-1}). When stars and gas are included, the gas tends to follow the stellar distribution, thus the pattern speeds of the gaseous spiral arms are higher ($5 - 17$ km s^{-1} kpc^{-1}).

These calculations may be improved by using a more consistent initial galaxy set up (e.g., Kuijken & Dubinski 1995). A natural extension of this work would also be to compare with observations by applying the Tremaine-Weinberg (Tremaine & Weinberg 1984) method to these calculations (see also Meidt et al. 2008b).

Acknowledgements. The calculations presented in these proceedings were performed using the University of Exeter's SGI Altix ICE 8200 supercomputer, Zen.

References

Bate, M. R., Bonnell, I. A., & Price, N. M. 1995, MNRAS, 277, 362
Bottema, R. 2003, MNRAS, 344, 358
Clemens, M. S., & Alexander, P. 2001, MNRAS, 321, 103
Dias, W. S., & Lépine, R. D. 2005, ApJ, 629, 831
Grosbøl, P., Dottori, H., & Gredel, R. 2004, A&A, 453, L25
Kormendy, J., & Norman, C. A. 1979, ApJ, 233, 539
Kuijken, K., & Dubinski, J. 1995, MNRAS, 277, 1341
Meidt, S. E., Rand, R. J., Merrifield, M. R., Debattista, V. P., & Shen, J. 2008a, ApJ, 676, 899
Meidt, S. E., Rand, R. J., Merrifield, M. R., Shetty, R., & Vogel, S. N. 2008b, ApJ, 688, 224
Oh, S. H., Kim, W.-T., Lee, H. M., & Kim, J. 2008, ApJ, 683, 94
Toomre, A., & Toomre, J. 1972, ApJ, 178, 623
Tremaine, S., & Weinberg, M. D. 1984, ApJ, 282, L5